JOURNAL OF GEOPHYSICAL RESEARCH, VOL. 112, D09117, doi:10.1029/2006JD007505, 2007

Observational estimates of radiative forcing due to land use change in southwest Australia

Udaysankar S. Nair,[1] Deepak K. Ray,[2,3] Jun Wang,[2,4] Sundar A. Christopher,[2] Tom J. Lyons,[5] Ronald M. Welch,[2] and R. A. Pielke Sr.[6]

Received 12 May 2006; revised 20 September 2006; accepted 22 November 2006; published 15 May 2007.

[1] Radiative forcing associated with land use change is largely derived from global circulation models (GCM), and the accuracy of these estimates depends on the robustness of the vegetation characterization used in the GCMs. In this study, we use observations from the Clouds and Earth's Radiant Energy System (CERES) instrument on board the Terra satellite to report top-of-the-atmosphere (TOA) radiative forcing values associated with clearing of native vegetation for agricultural purposes in southwest Australia. Over agricultural areas, observations show consistently higher shortwave fluxes at the TOA compared to native vegetation, especially during the time period between harvest and planting. Estimates using CERES observations show that over a specific area originally covered by native vegetation, replacement of half the area by croplands results in a diurnally averaged shortwave radiative forcing of approximately -7 W m^{-2}. GCM-derived estimates for areas with 30% or more croplands range from -1 to -2 W m^{-2} compared to observational estimate of -4.2 W m^{-2}, thus significantly underestimating radiative forcing due to land use change by a factor of 2 or more. Two potential reasons for this underestimation are incorrect specification of the multiyear land use change scenario and the inaccurate prescription of seasonal cycles of crops in GCMs.

Citation: Nair, U. S., D. K. Ray, J. Wang, S. A. Christopher, T. J. Lyons, R. M. Welch, and R. A. Pielke Sr. (2007), Observational estimates of radiative forcing due to land use change in southwest Australia, *J. Geophys. Res.*, *112*, D09117, doi:10.1029/2006JD007505.

1. Introduction

[2] In the past three decades, there has been considerable research into understanding and quantifying anthropogenic influences on Earth's climate. Of significant interest is the impact of steady increases in the concentrations of absorbing trace gases in the atmosphere, especially carbon dioxide, resulting in a reduction in the net outgoing longwave radiation from the Earth-atmosphere system and thereby leading to an increase in surface temperatures. However, there are other effects that have the potential to amplify or mask this warming. Positive feedback effects, such as an increase in atmospheric water vapor, result in increased surface temperatures, while negative feedback effects, such as increases in low-level cloudiness and aerosols from natural and anthropogenic influences, lead to reductions in surface temperatures [*Hansen et al.*, 1998; *Committee on Radiative Forcing Effects on Climate Change*, 2005].

[3] Radiative forcing, the change in the net outgoing flux in response to a perturbation to the climate system, is a concept that is useful for comparing the relative importance of the different mechanisms that affect climate change [*Houghton et al.*, 1995; *Betts*, 2001]. A significant amount of research has been devoted to estimate the magnitude of radiative forcing associated with anthropogenic perturbations in atmospheric greenhouse gases, aerosols and high-level clouds. However, land surface characteristics also have been subject to drastic changes [e.g., *Klein Goldewijk*, 2001]. Because of the demand for forest products, tropical deforestation has proceeded quite rapidly, with the low albedo forests replaced by pastures and croplands of relatively higher albedo, thereby leading to changes in radiative forcing [*Nobre et al.*, 2004].

[4] Radiative forcing associated with human-induced land use change has been derived largely from General Circulation Model (GCM) simulations. *Hansen et al.* [1998] used climate simulations for preindustrial and current land use scenarios, from which they estimated a radiative forcing of -0.21 W m^{-2} and a global reduction in surface temperature of 0.14 K. Recently, *Betts* [2001] conducted 20-year climate simulations for preindustrial and current land use scenarios using the Hadley Center General Circulation model

[1] Earth System Science Center, National Space Science and Technology Center, University of Alabama, Huntsville, Alabama, USA.
[2] Department of Atmospheric Sciences, University of Alabama, Huntsville, Alabama, USA.
[3] Now at Forestry and Natural Resources, Purdue University, West Lafayette, Indiana, USA.
[4] Now at Division of Engineering and Applied Science, Harvard University, Cambridge, Massachusetts, USA.
[5] School of Environmental Science, Murdoch University, Murdoch, Western Australia, Australia.
[6] Department of Atmospheric Science, Colorado State University, Fort Collins, Colorado, USA.

0148-0227/07/2006JD007505$09.00

(HadAM3) at 3.5° longitude and 2.5° latitude resolutions. A radiative forcing of -0.2 W m^{-2} was reported, with an annual mean global temperature decrease of about 0.02 K.

[5] The estimates of radiative forcing derived from GCM simulations by *Hansen et al.* [1998] and *Betts* [2001] are subject to assumptions made about the land cover distribution, temporal variations in albedo for various types of vegetation, and modulating influences such as grid spacing, snow cover and soil moisture. Indeed, *Hansen et al.* [1998] assumed that the albedo of croplands is similar to that of grasslands, and that the albedo for regrowth in formerly deforested tropical forests is comparable to that of woodlands. However, cropland albedo may be significantly different from grassland albedo, depending on the type of cultivation. For example *Gao et al.* [2005] reported global average minimum and maximum broadband albedo values of (0.159, 0.327) for grasslands and (0.131,0.231) for croplands, respectively. The albedos vary seasonally because of land management practices with crops and are associated with the phenology of the natural grasslands. The albedo of regrowth in deforested tropical areas can attain values characteristic of undisturbed conditions in relatively short timescales [*Bruijnzeel*, 2004]. The *Betts* [2001] simulations resolved only human-induced land surface changes that cover an area 25% or more of each grid cell, and snow cover significantly impacts the albedo of croplands compared to forested areas. Hence, for the same type of vegetation, different albedos are prescribed for snowy and snow-free conditions [*Hansen et al.*, 1998; *Betts*, 2001]. Furthermore, bare soil albedo is a function of soil moisture in GCMs, and parameterized precipitation processes have a significant modulation effect on the radiative forcing estimates derived from the GCMs.

[6] To our knowledge, there are very few observational estimates of radiative forcing associated with land use change [*Myhre et al.*, 2005]. The *Committee on Radiative Forcing Effects on Climate Change* [2005] report summarizes the understanding of the global averaged forcing of the albedo change due to landscape change as follows: The *Intergovernmental Panel on Climate Change* [2001] reports the global-averaged forcing due to albedo change alone as -0.25 ± 0.25 W m^{-2}. The level of scientific understanding is listed as "very low." The uncertainties in the albedo change reflect the complexity of the land surface (e.g., type of vegetation, phenology, density of coverage, soil color). When aggregating regional information about land surface with these uncertainties up to the global scale, large global average uncertainty ranges still result as there is no reason to expect these uncertainties are random across landscape types. A recent assessment of the radiative impact of albedo change estimates a range of -0.6 to 0.5 W m^{-2}, with the negative values being more likely [*Myhre and Myhre*, 2003].

[7] Satellite observations provide an ideal tool to diagnose radiative forcing due to land use changes, but deriving global estimates from this source is limited since the observations do not extend prior to the 1970s. Nevertheless, it is possible to obtain regional estimates over areas where sizable, adjacent tracts of natural and altered landscapes exist. One example is southwest Australia, where 13 million hectares of native vegetation has been cleared to make way for agriculture. It offers the opportunity to obtain observational estimates of radiative forcing caused by land use that is comparable to the simulations of *Betts* [2001] and *Hansen et al.* [1998].

2. Data and Area of Study

[8] The Single Satellite Footprint (SSF) product, which includes the TOA and surface fluxes along with cloud information (version 2B) derived from the Clouds and Earth's Radiant Energy System (CERES) instrument [*Wielicki et al.*, 1996], is utilized in this study. The CERES instrument makes broadband measurements of TOA radiances at 0.3 to >50 μm, 0.3–5 μm (shortwave) and 8–12 μm (longwave), all at 20 km nadir spatial resolution. The SSF data set is derived by combining instantaneous CERES sensor observations with information from the Moderate Resolution Imaging Spectroradiometer (MODIS). The broadband radiances are converted to TOA fluxes using empirical angular models [*Loeb et al.*, 2005]. Cloudiness information from the MODIS sensor in the SSF data set is used to identify CERES footprints for clear conditions, while the International Geosphere-Biosphere Program (IGBP) ecosystem database [*Prince et al.*, 1995] is used determine associated land use types. The SSF data used in this study is for the time period 2000–2003, obtained from the CERES instrument aboard the Terra satellite.

[9] The area of interest in Southwest Australia is between 31–33.5°S and 117.625–121.375°E (Figure 1). This region has experienced drastic changes in land use in the past few decades, with approximately thirteen million hectares of native vegetation in this region being replaced by winter-growing agricultural species. A 750 km long vermin-proof fence demarcates the croplands in the west from the native vegetation to the east, and this boundary is conspicuous even in medium resolution satellite imagery because of the stark difference in albedo between the croplands and native vegetation (Figure 1). Land use changes in the study area, of the type discussed in this paper, should be expected to occur with respect to future land use changes around the globe, whenever the replacement of native vegetation cover by croplands or urban development occurs [*Australia Conservation Foundation*, 2001].

[10] The present study focuses on an area that is approximately covered by equal proportions of native vegetation and croplands. The size of this area is about the same as the grid cell in the numerical simulations by *Betts* [2001].

3. Methodology

[11] We examine the seasonal variation of TOA cloud-free diurnally averaged shortwave radiative forcing due to anthropogenic land use change using the CERES SSF observations. The data at the time of the satellite overpass (called instantaneous) is used in this study, and these values are converted to diurnal average values, as described in section 4.1. The IGBP ecosystem information provided in the SSF data set is used to isolate CERES footprints in the study area that are located over agriculture and native vegetation. The native vegetation and agricultural areas are classified as Croplands and Woody Savanna, respectively, in the IGBP classification method. The cloud mask flag derived from MODIS in the SSF data set then is used to

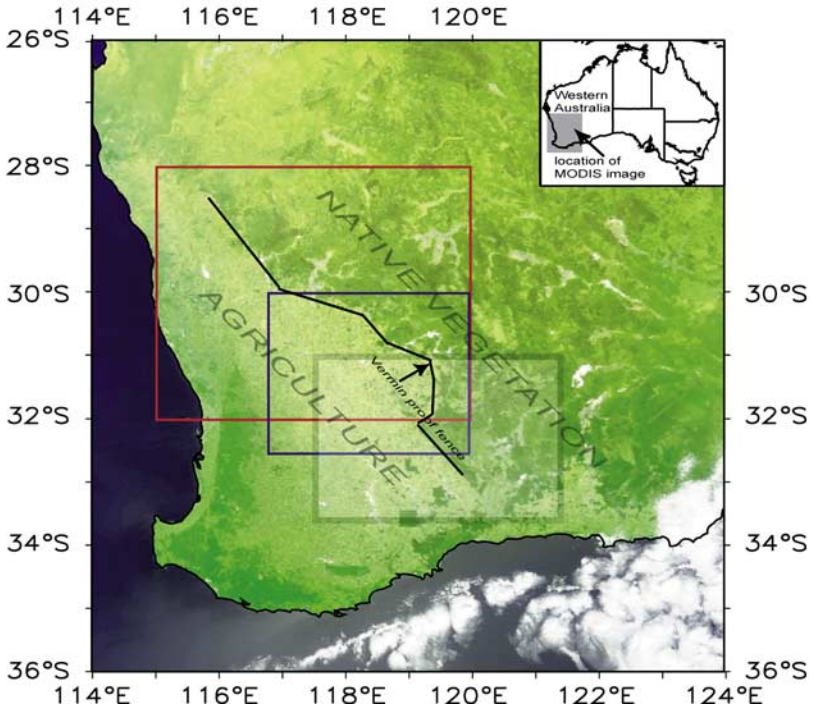

Figure 1. MODIS three channel color composite over southwest Australia. The area of interest in this study is highlighted by the shaded box. The locations of the GCM grid cells from *Hansen et al.* [1998] and *Betts* [2001] used for comparison against observations are shown using red and blue boxes, respectively.

discriminate between clear and cloudy CERES footprints. The monthly mean upwelling shortwave, longwave and net radiative fluxes at the TOA and the surface then are computed for clear-sky conditions as a function of land use for the time period of 2000–2003.

[12] The CERES and MODIS observations are obtained during the time of the satellite overpass which is approximately at 1030 local time. However, to compare these results to other studies, diurnal averaging is needed. We define the ratio between the diurnally averaged flux and instantaneous flux as a scaling factor α

$$\alpha(\mu_{obs}) = \frac{\int_{\mu_{sunrise}}^{\mu_{sunset}} F(\mu)d\mu}{2F(\mu_{obs})}, \qquad (1)$$

where F(μ) is upwelling solar flux at the TOA when the cosine of solar zenith angle is equal to μ; μ_{sunset}, μ_{sunrise}, and μ_{obs}, are the cosine of solar zenith angles at sun rise, sun set and CERES observation time, respectively. The time is expressed in terms of μ; thus 24 hours are equivalent to a value of 2 in cosine coordinates.

[13] In this study, we use a delta four-stream radiative transfer model (hereafter δ-4S RTM) to compute the F(μ) and the scaling factor α. The δ-4S RTM is a plane-parallel broadband radiative transfer model, originally designed to calculate the radiative flux at the TOA and the surface in clear and cloudy conditions [*Fu and Liou*, 1993], that was later modified for calculation of radiative effect of aerosols, such as smoke [*Christopher et al.*, 2000] and dust [*Wang et al.*, 2004]. The model divides the shortwave (SW) spectrum ($0.2 \sim 4$ μm) into 6 bands and the longwave (LW) spectrum ($4 \sim 35.7$ μm) into 12 bands. To treat the radiative transfer accurately, the δ-4S RTM uses a δ-function to better represent the phase function in the forward scattering direction [*Liou et al.*, 1988]. Rayleigh scattering, together with gas absorption and water vapor absorption (using the correlated k-distribution method), are included in the model calculations. For the principal atmospheric gases, the difference between the δ-4S RTM and line-by-line irradiance calculations is within 0.05% [*Fu and Liou*, 1993]. Our recent studies indicate an excellent agreement between calculated and observed downward shortwave irradiances at the surface, with differences of less than 3% when aerosol effects are carefully considered in the calculations [*Wang et al.*, 2003; *Christopher et al.*, 2003]. While calculating F(μ) and α, we used the CERES surface spectral reflectance (R_s) of woody savanna and croplands outlined by *Charlock et al.* [1997]. On the basis of the latitude and longitude in the study region, the variations of μ_{sunset} and μ_{sunrise} as a function of time also are considered in the calculations. Given the solar zenith angle (μ_{obs}) at the satellite-observation time, the scaling factor $\alpha(\mu_{\text{obs}})$ is calculated using equation (1) and the δ-4S RTM. The diurnally averaged flux is then obtained by scaling the CERES observed instantaneous flux (F_{CERES}) by $\alpha(\mu_{\text{obs}})$.

4. Results

4.1. Seasonal Variation of Instantaneous Upwelling Shortwave Flux at the TOA

[14] There are significant and consistent differences in monthly averaged instantaneous cloud-free upwelling shortwave fluxes at the TOA between agricultural and native vegetation areas (Figure 2). The maximum and minimum

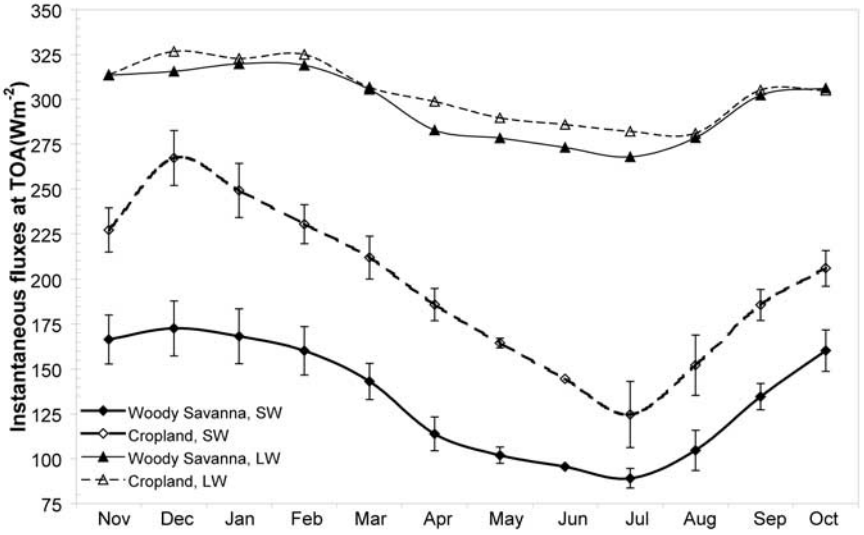

Figure 2. Seasonal variations in monthly averaged upwelling longwave and shortwave fluxes at the TOA for the 2000–2003 time periods. Longwave fluxes over native vegetation and agricultural areas are show using solid and dashed lines, respectively.

values for both ecosystems are observed during the months of January and June, which are the southern hemisphere summer and winter months, respectively. The seasonal variations of upwelling shortwave fluxes at the TOA are governed both by changes in surface albedo and solar declination. Previous studies [*Ray et al.*, 2003] suggest that there is significantly less seasonal variation in surface albedo over the native vegetation areas compared to croplands. Analysis of Normalized Difference Vegetation Index (NDVI), a satellite-derived indicator of surface vegetation, shows relatively constant values over native vegetation areas, while varying by a factor of 2 over agricultural areas [*Ray et al.*, 2003]. In agricultural areas, crops that are planted in April become mature during the months of August–October and are harvested between November–December. The seasonal variations in instantaneous upwelling shortwave fluxes at the TOA reflect these differences between agricultural and native vegetation areas. Throughout the annual cycle, the upwelling shortwave fluxes are higher over the agricultural areas compared to native vegetation, with the smallest differences found during the early growing season month (July) with a value of 35.5 W m^{-2} (Figure 3). During the mature growth stage of the crops, spanning August–October, differences in upwelling shortwave fluxes remain relatively constant, about 50 W m^{-2} (Figure 3). During November, the differences in instantaneous fluxes increase to about 60 W m^{-2} in response to the drying of the crops and the onset of harvesting. In response to exposing bare soil following harvest the differences reach a maximum of 94.6 W m^{-2} in December. After harvest, the differences decrease to a value of approximately 70 W m^{-2} and then remain nearly constant until April after which they steadily decrease until July.

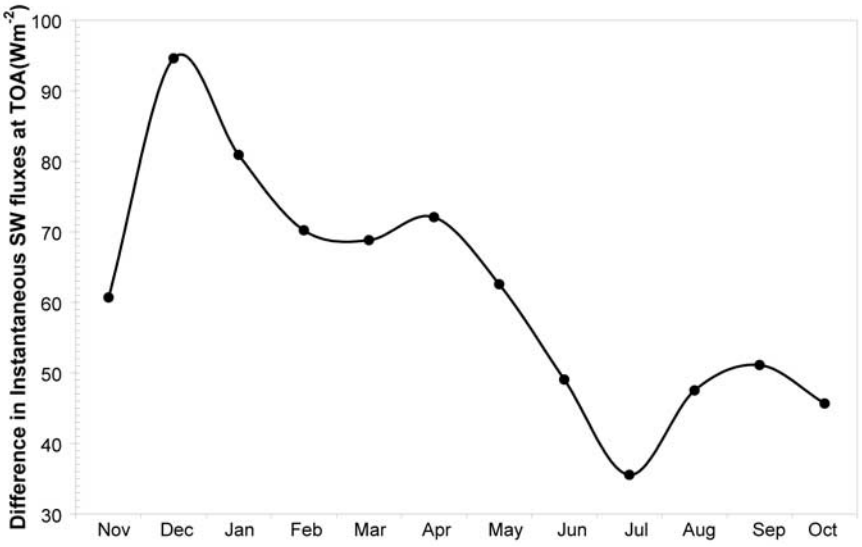

Figure 3. Differences in monthly averaged upwelling shortwave fluxes at the TOA between native vegetation and agricultural areas for the 2000–2003 time periods.

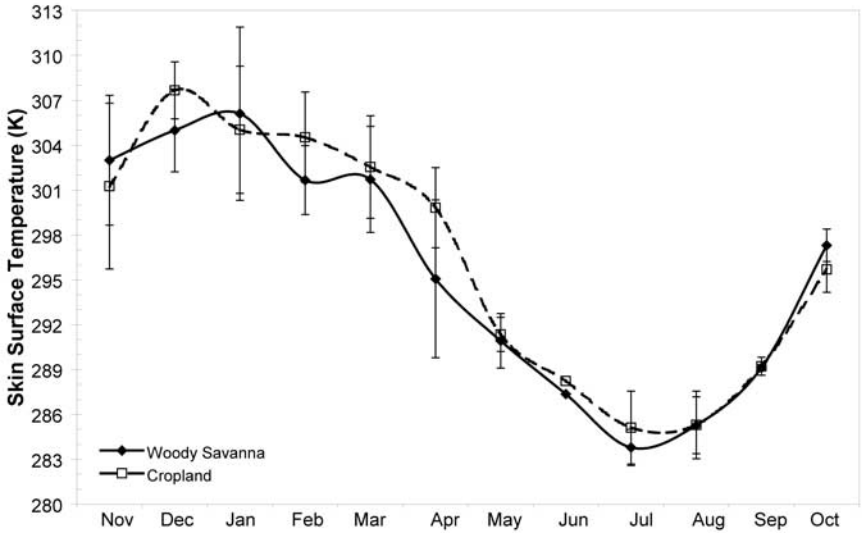

Figure 4. Seasonal variations in monthly averaged land surface temperature for the 2000–2003 time periods. Values over native vegetation and agricultural areas are shown using solid and dashed lines, respectively.

4.2. Seasonal Variations in Cloud-Free Sky Upwelling Longwave Fluxes at the TOA

[15] Seasonal differences in cloud-free upwelling longwave fluxes at the TOA between native vegetation and croplands (Figure 2) are relatively small. During the growing season months ranging from July–October, the upwelling longwave fluxes at the TOA are higher over the agricultural areas. The maximum differences during the growing season occur in July and then progressively decrease, reaching an almost zero value by October. The upwelling longwave fluxes at the TOA become higher over agricultural areas by about 12 W m^{-2} after harvest in December and then remain approximately constant over both ecosystems until April, when they again become higher over agricultural areas. Seasonal variations in land surface temperatures (LST) of the agricultural and native vegetation areas (Figure 4) suggest that the differences in land use do not play an important role in determining the upwelling longwave at the TOA. Note that the differences in upwelling longwave at TOA is maximum during the April–July time period, but the differences in surface temperature is least during this period with the exception of the month of April.

[16] The seasonal variation of cloud-free instantaneous net radiative fluxes at the TOA (not shown) is primarily governed by seasonal variations in upwelling shortwave fluxes at the TOA. The instantaneous net radiative fluxes at the TOA are consistently higher over native vegetation areas throughout the year (not shown). Differences in net radiative fluxes are relatively constant during the agricultural growing season and then increase after harvest. Note that even though the net fluxes at the TOA are higher over native vegetation areas, especially after harvest, the average LST values over the native vegetation areas are smaller compared to cropland values (Figure 4). This is due to differences in turbulent transfer of heat and moisture from the land surface [*Smith et al.*, 1992]. Owing to higher roughness over native vegetation areas, the boundary layer turbulent heat and moisture transport is more efficient. In addition, transpiration from vegetation leads to utilization of a part of the incoming shortwave for evaporation of water in the native vegetation area, while most of it is utilized for heating the land surface in the bare agricultural areas. During the mature stages of crop growth, the LSTs over croplands are slightly smaller compared to native vegetation areas. This could be due to more efficient transpiration by crop species in the mature stages of their growth.

4.3. Seasonal Variation of Diurnally Averaged Upwelling Shortwave at the TOA

[17] The diurnally averaged upwelling shortwave fluxes at the TOA, computed using equation (1), show consistent differences between the native vegetation and agricultural areas, with higher values over agricultural areas (Figure 5). A minimum difference of approximately 10 W m^{-2} is observed between the native vegetation and agricultural areas earlier in the growing season, steadily increasing in magnitude as the crops mature, and then remaining approximately constant at 30 W m^{-2}. The annual means of the diurnally averaged upwelling shortwave fluxes for the native vegetation ($\overline{F}_{native}$) and agricultural areas ($\overline{F}_{crop}$) are approximately 51 W m^{-2} and 75 W m^{-2}, respectively. The mean annual shortwave radiative forcing resulting from the land use change ($\Delta\overline{F}_{landuse}$) is computed as a function of the fractional area of native vegetation replaced by the croplands (f_{crop}), using the following expression:

$$\begin{aligned}\Delta\bar{F}_{landuse} &= \bar{F}_{native} - \left[(1-f_{crop})\bar{F}_{native} + f_{crop}\bar{F}_{crop}\right] \\ &= \left[\bar{F}_{native} - \bar{F}_{crop}\right]f_{crop} \end{aligned} \quad (2)$$

The mean annual shortwave radiative forcing varies from -1.4 W m^{-2} to -13.9 W m^{-2} for values of f_{crop} ranging from 0.1 to 1 (Table 1). In the study area, which was originally completely covered by native vegetation, approximately half of the area has been cleared for agricultural purposes. Using a value of 0.5 for f_{crop}, the mean annual shortwave radiative forcing due to land use change in the study area is

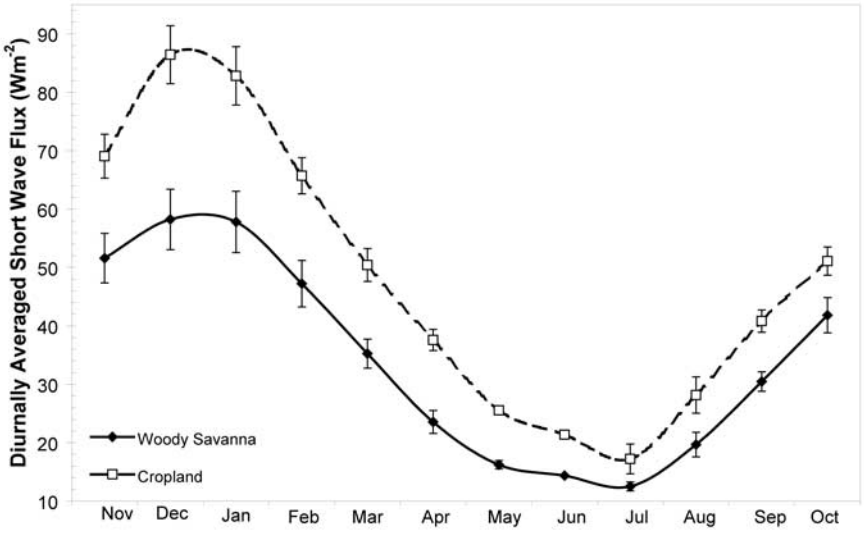

Figure 5. Seasonal variations in monthly mean, diurnally averaged upwelling shortwave at the top-of-the-atmosphere for the 2000–2003 time periods. Values over native vegetation and agricultural areas are show using solid and dashed lines, respectively.

-7.0 W m^{-2}. In the GCM used by *Hansen et al.* [1998] the grid cell, with a center location of 30°S, 117.5°E and extending 4° × 5° in latitude and longitude, respectively, straddles the agricultural and native vegetation area in southwest Australia (Figure 1). On the basis of the IGBP land use data set, 30% of this grid cell is made up of land use types that are associated with anthropogenic activities. The GCM derived estimate of net radiative forcing for this grid cell is -2.038 W m^{-2} which is a factor of 2 less than the mean annual shortwave forcing of -4.2 W m^{-2} estimated for $f_{crop} = 0.3$. Note that when comparing the net radiative forcing reported by *Hansen et al.* [1998] against the observational estimate of shortwave radiative forcing, it is assumed that the net radiative forcing is dominated by the shortwave component. The discussion in section 4.2, showing that the land use differences do not significantly impact the top-of-the-atmosphere longwave fluxes, supports this assumption. *Betts* [2001] reports GCM-derived shortwave radiative forcing estimates in the range of -1 to -2 W m^{-2}. The approximate location of the grid cell from the *Betts* [2001] study is shown in Figure 1. The f_{crop} value for this grid cell exceeds 0.3, and thus the GCM estimated range is at least 2 times less than the CERES estimated value of -4.2 W m^{-2}. Comparisons with observational estimates over the study area show that the GCM computations significantly underestimate the shortwave radiative forcing due to land use change.

4.4. Uncertainty Analysis

[18] The accuracy of our results presented here relies on the uncertainties in CERES instantaneous fluxes, F_{CERES}, as well as the scaling factor α used for converting F_{CERES} into diurnally averaged values of $\overline{F}$. On the basis of CERES radiance measurements, the regional instantaneous TOA fluxes in cloud-free sky conditions are estimated to be <8.7 W m^{-2} in the SW and <2.4 W m^{-2} in the LW [cf. *Loeb et al.*, 2003, Table 2]. The monthly averages of instantaneous TOA SW and LW fluxes both have an uncertainty less than 2 W m^{-2} [*Loeb et al.*, 2003, Table 6], and the uncertainties in seasonal or annual flux averages are less than 1 W m^{-2} [*Wielicki et al.*, 2005]. It should be noted, however, the averages of instantaneous fluxes cannot be directly used to derive the actual radiative energy budget, unless the diurnal variation of fluxes or diurnal scaling factor showed in equation (1) is taken into account. Since all values (including $F(\mu_{obs})$) in equation (1) are computed from the δ-4S RTM, the numerator and denominator have the same systemic errors, and when the ratio α is calculated, those errors largely cancel. As a result, the uncertainties of solar zenith on atmospheric optical conditions (e.g., air mass or Rayleigh optical thickness change as a function of μ), which is one of the difficulties in converting F_{CERES} to the diurnally averaged values, are minimized. Our sensitivity analysis shows that a ±10% change in surface albedo used in the δ-4S RTM leads to changes in the scaling factor of ±1%. If we assume the mean F_{CERES} to be 150 W m^{-2}, the total uncertainties (from scaling factor and other uncertainties) in our analysis are less than ±1.5 W m^{-2}, values

Table 1. Shortwave Radiative Forcing Due to Land Use Change as a Function of Land Area Fraction Cleared for Agricultural Purposes Where f_{crop} Is Percent Land Area Cleared and $\Delta\overline{F}_{landuse}$ Is Shortwave Radiative Forcing

f_{crop}	$\Delta\overline{F}_{landuse}$, W m^{-2}
0.1	−1.4
0.2	−2.8
0.3	−4.2
0.4	−5.6
0.5	−7.0
0.6	−8.4
0.7	−9.8
0.8	−11.2
0.9	−12.6
1.0	−13.9

smaller than the differences found between the observation-based and GCM-calculated land use forcing.

5. Summary

[19] Radiative forcing associated with human-induced land use changes is not well understood, and the estimates that were used in the 2001 Intergovernmental Panel on Climate Change (IPCC) were derived from numerical models. This study examines the seasonal variation of the TOA radiative fluxes as a function of land use in the southwest Australian region, a site in which large tracts of native vegetation have been cleared for agricultural purposes. The annual cycle of shortwave fluxes at the TOA show significant differences between native vegetation areas and croplands, especially during the time period between harvest and planting. However, instantaneous longwave fluxes at the TOA do not differ significantly. Comparison of annual mean diurnally averaged shortwave fluxes estimated from CERES observations and GCM simulations [*Hansen et al.*, 1998; *Betts*, 2001] show significant differences (-4 W m^{-2} versus -2 W m^{-2}) over southwest Australia. Observational estimates are more than twice the model-derived values over this region even when observational uncertainties are taken into account. *Betts* [2001] and *Hansen et al.* [1998] both report that the radiative forcing due to land use change is most significant in the midlatitude agricultural areas that experience snowfall, which accentuates the albedo effect associated conversion of forests to farm lands. The present analysis suggests that shortwave radiative forcing associated with agricultural land use may be significant even in areas without frequent snow cover. Previous studies by *Ray et al.* [2003] over southwest Australia, however, show that clouds tend to form more over native vegetation and thus may partially offset the direct forcing as a negative feedback.

[20] The differences in CERES observed and GCM-derived estimates of radiative forcing may be due to (1) the use of incorrect land use change scenarios and (2) inadequate prescription of the seasonal cycle of variations in cropland vegetation characteristics within GCMs. The majority of the numerical models use a single predefined temporal behavior for vegetation characteristics, such as fractional vegetation cover and leaf area index associated with a particular land use category. While such specification may be adequate for natural vegetation, the temporal behavior of vegetative characteristics associated with agricultural crops may differ drastically depending upon the types of crop, geographic area and agricultural practices. For example in southwest Australia the fields remain bare during the summer and early fall since the crops are winter rain fed. However, in other geographical areas with longer growing seasons and higher water availability, the fields may remain barren for much shorter periods of time. Vegetation parameterizations in regional and global weather and climate models need to account for these types of differences in order to better represent the surface radiative energy budget over land areas altered by human activity.

[21] **Acknowledgments.** This work was funded by National Science Foundation grant ATM-0523583 and the Australian Research Council's Discovery funding scheme (project DP0664515). D. Ray was supported by a NASA ESS graduate student fellowship. J. Wang was supported by the NASA ESS graduate student fellowship, and while at Harvard, his work was supported by the NOAA Climate and Global Change postdoctoral fellowship under the administration of UCAR visiting scientist program. Sundar A. Christopher was supported by NASA's Radiation and Interdisciplinary Science Programs. The authors are thankful to Jim Hansen and Makiko Sato for providing information on the GCM simulated radiative forcing.

References

Australia Conservation Foundation (2001), *Australian Land Clearing, A Global Perspective: Latest Facts and Figures*, Aust. Conserv. Found., Fitzroy, Vic., Australia.

Betts, R. (2001), Biogeophysical impacts of land use on present-day climate: Near-surface temperature and radiative forcing, *Atmos. Sci. Lett.*, *2*, 39–51, doi:10.1006/asle.2000.0023.

Bruijnzeel, L. A. (2004), Hydrological functions of tropical forests: Not seeing the soil for the trees?, *Agric. Ecosyst. Environ.*, *104*, 185–228.

Charlock, T. P., et al. (1997), Compute surface and atmospheric fluxes (system 5.0): CERES Algorithm Theoretical Basis Document Release 2.2, *NASA/RP-1376*, 84 pp., NASA Langley Res. Cent., Hampton, Va. (Available at http://asd-www.larc.nasa.gov/ATBD/ATBD.html)

Christopher, S. A., X. Li, R. M. Welch, P. V. Hobbs, J. S. Reid, and T. F. Eck (2000), Estimation of downward and top-of-atmosphere shortwave irradiances in biomass burning regions during SCAR-B, *J. Appl. Meteorol.*, *39*, 1742–1753.

Christopher, S. A., J. Wang, Q. Ji, and S.-C. Tsay (2003), Estimation of diurnal shortwave dust aerosol radiative forcing during PRIDE, *J. Geophys. Res.*, *108*(D19), 8596, doi:10.1029/2002JD002787.

Committee on Radiative Forcing Effects on Climate Change (2005), *Radiative Forcing of Climate Change: Expanding the Concept and Addressing Uncertainties*, 224 pp., Clim. Res. Comm., Board on Atmos. Sci and Clim., Div. on Earth and Life Studies, Natl. Res. Council., Natl. Acad., Washington, D. C.

Fu, Q., and K. N. Liou (1993), Parameterization of the radiative properties of cirrus clouds, *J. Atmos. Sci.*, *50*, 2008–2025.

Gao, F., C. B. Schaaf, A. H. Strahler, A. Roesch, W. Lucht, and R. Dickinson (2005), MODIS bidirectional reflectance distribution function and albedo Climate Modeling Grid products and the variability of albedo for major global vegetation types, *J. Geophys. Res.*, *110*, D01104, doi:10.1029/2004JD005190.

Hansen, J., M. Sato, A. Lacis, R. Ruedy, I. Tegen, and E. Matthews (1998), Climate forcings in the Industrial Era, *Proc. Natl. Acad. Sci. U. S. A.*, *95*, 12,753–12,758.

Houghton, J. T., L. G. M. Filho, J. Bruce, H. Lee, B. A. Callander, E. Haites, N. Harris, and K. Maskell (1995), *Climate Change 1994: Radiative Forcing of Climate Change*, Cambridge Univ. Press, New York.

Intergovernmental Panel on Climate Change (IPCC) (2001), *Climate Change 2001: The Scientific Basis: Contribution of Working Group I to the Third Assessment Report of the Intergovernmental Panel on Climate Change*, edited by J. T. Houghton et al., 881 pp., Cambridge Univ. Press, New York.

Klein Goldewijk, K. (2001), Estimating global land use change over the past 300 years: The HYDE database, *Global Biogeochem. Cycles*, *15*, 417–434.

Liou, K. N., Q. Fu, and T. P. Ackerman (1988), A simple formulation of the d-four-stream approximation for radiative transfer parameterizations, *J. Atmos. Sci.*, *45*, 1940–1947.

Loeb, N. G., N. M. Smith, S. Kato, W. F. Miller, S. K. Gupta, P. Minnis, and B. A. Wielicki (2003), Angular distribution models for top-of-atmosphere radiative flux estimation from the clouds and the Earth's energy system instrument on the TRMM satellite. Part I: Methodology, *J. Appl. Meteorol.*, *42*, 240–265.

Loeb, N. G., S. Kato, K. Loukachine, and N. M. Smith (2005), Angular distribution models for top-of-atmosphere radiative flux estimation from the clouds and the Earth's radiant energy system instrument on the Terra satellite. Part I: Methodology, *J. Atmos. Oceanic Technol.*, *22*, 338–351.

Myhre, G., and A. Myhre (2003), Uncertainties in radiative forcing due to surface albedo changes caused by land-use changes, *J. Clim.*, *16*, 1511–1524.

Myhre, G., M. M. Kvalevåg, and C. B. Schaaf (2005), Radiative forcing due to anthropogenic vegetation change based on MODIS surface albedo data, *Geophys. Res. Lett.*, *32*, L21410, doi:10.1029/2005GL024004.

Nobre, C. A., et al. (2004), The Amazonian climate, in *Vegetation, Water, Humans and the Climate: A New Perspective on an Interactive System*, chap. 6, edited by P. Kabat et al., 566 pp., Springer, New York.

Prince, S. D., R. J. Olson, G. Dedieu, G. Esser, and W. Cramer (1995), Global primary production land data initiative project description, *IGBP-DIS Working Paper 12*, Int. Geosphere and Biosphere Programme-DIS, Paris.

Ray, D. K., U. S. Nair, R. M. Welch, Q. Han, J. Zeng, W. Su, T. Kikuchi, and T. J. Lyons (2003), Effects of land use in Southwest Australia:

1. Observations of cumulus cloudiness and energy fluxes, *J. Geophys. Res.*, *108*(D14), 4414, doi:10.1029/2002JD002654.

Smith, R. C. G., H. Xinmei, T. J. Lyons, J. M. Hacker, and P. T. Hick (1992), Change in land surface albedo and temperature in southwestern Australia following replacement of perennial vegetation by agriculture: Satellite observations, World Space Congress 2992, 43rd Congress of the International Astronautical Federation, *IAF Paper IAF-92-0117*, Int. Astronaut. Fed., Washington D. C.

Wang, J., S. A. Christopher, J. S. Reid, H. Maring, D. Savoie, B. N. Holben, J. M. Livingston, P. B. Russell, and S. Yang (2003), GOES 8 retrieval of dust aerosol optical thickness over the Atlantic Ocean during PRIDE, *J. Geophys. Res.*, *108*(D19), 8595, doi:10.1029/2002JD002494.

Wang, J., U. Nair, and S. A. Christopher (2004), GOES-8 aerosol optical thickness assimilation in a mesoscale model: Online integration of aerosol radiative effects, *J. Geophys. Res.*, *109*, D23203, doi:10.1029/2004JD004827.

Wielicki, B. A., B. R. Barkstrom, E. F. Harrison, R. B. Lee III, G. L. Smith, and J. E. Cooper (1996), Clouds and the Earth's Radiant Energy System (CERES): An Earth observing system experiment, *Bull. Am. Meteorol. Soc.*, *77*, 853–868.

Wielicki, B. A., T. Wong, N. Loeb, P. Minnis, K. Priestley, and R. Kandel (2005), Changes in Earth's albedo measured by satellite, *Science*, *308*, 825.

S. A. Christopher and R. M. Welch, Department of Atmospheric Sciences, University of Alabama, Huntsville, AL 35806, USA.

T. J. Lyons, School of Environmental Science, Murdoch University, South Street, Murdoch, WA 6150, Australia.

U. S. Nair, Earth System Science Center, National Space Science and Technology Center, University of Alabama, Huntsville, AL 35806, USA. (nair@nsstc.uah.edu)

R. A. Pielke Sr., Department of Atmospheric Science, Colorado State University, Fort Collins, CO 80523, USA.

D. K. Ray, Forestry and Natural Resources, Purdue University, West Lafayette, IN 47907, USA.

J. Wang, Division of Engineering and Applied Science, Harvard University, 29 Oxford Street, Cambridge, MA 02474, USA.